Kinetic and Pharmacological Properties of $GABA_A$ Receptors in Single Thalamic Neurons and $GABA_A$ Subunit Expression

S. H. BROWNE,[1,*] J. KANG,[2,*] G. AKK,[2] L. W. CHIANG,[1] H. SCHULMAN,[1] J. R. HUGUENARD,[2] AND D. A. PRINCE[2]

[1]*Department of Neurobiology and* [2]*Department of Neurology and Neurological Sciences, Stanford University School of Medicine, Stanford, California 94305-5122*

Received 8 November 2000; accepted in final form 31 July 2001

Browne, S. H., J. Kang, G. Akk, L. W. Chiang, H. Schulman, J. R. Huguenard, and D. A. Prince. Kinetic and pharmacological properties of $GABA_A$ receptors in single thalamic neurons and $GABA_A$ subunit expression. *J Neurophysiol* 86: 2312–2322, 2001. Synaptic inhibition in the thalamus plays critical roles in sensory processing and thalamocortical rhythm generation. To determine kinetic, pharmacological, and structural properties of thalamic γ-aminobutyric acid type A ($GABA_A$) receptors, we used patch-clamp techniques and single-cell reverse transcriptase polymerase chain reaction (RT-PCR) in neurons from two principal rat thalamic nuclei—the reticular nucleus (nRt) and the ventrobasal (VB) complex. Single-channel recordings identified $GABA_A$ channels with densities threefold higher in VB than nRt neurons, and with mean open time fourfold longer for nRt than VB [14.6 ± 2.5 vs. 3.8 ± 0.7 (SE) ms, respectively]. $GABA_A$ receptors in nRt and VB cells were pharmacologically distinct. Zn^{2+} (100 μM) reduced $GABA_A$ channel activity in VB and nRt by 84 and 24%, respectively. Clonazepam (100 nM) increased inhibitory postsynaptic current (IPSC) decay time constants in nRt (from 44.3 to 77.9 ms, $P < 0.01$) but not in VB. Single-cell RT-PCR revealed subunit heterogeneity between nRt and VB cells. VB neurons expressed α1–α3, α5, β1–3, γ2–3, and δ, while nRt cells expressed α3, α5, γ2–3, and δ. Both cell types expressed more subunits than needed for a single receptor type, suggesting the possibility of $GABA_A$ receptor heterogeneity within individual thalamic neurons. β subunits were not detected in nRt cells, which is consistent with very low levels reported in previous in situ hybridization studies but inconsistent with the expected dependence of functional $GABA_A$ receptors on β subunits. Different single-channel open times likely underlie distinct IPSC decay time constants in VB and nRt cells. While we can make no conclusion regarding β subunits, our findings do support α subunits, possibly α1 versus α3, as structural determinants of channel deactivation kinetics and clonazepam sensitivity. As the γ2 and δ subunits previously implicated in Zn^{2+} sensitivity are both expressed in each cell type, the observed differential Zn^{2+} actions at VB versus nRt $GABA_A$ receptors may involve other subunit differences.

INTRODUCTION

The thalamus is both the gateway to the cerebral cortex and an information processing unit. Impulses arriving from sensory, motor, and even "limbic system" pathways are processed in specific thalamic relay nuclei and then transmitted to appropriate cortical areas. The nucleus reticularis (nRt) surrounds the thalamus like a shield. Fibers interconnecting thalamus and cortex traverse nRt and establish synapses on reticular neurons (Jones 1985). Reciprocal connections between relay nuclei and nRt provide an anatomic substrate for intrathalamic oscillations that occur during slow-wave sleep and the pathophysiological state of absence epilepsy (Huguenard 1999; Steriade et al. 1993). Recurrent inhibitory synapses between nRt neurons serve to control the output of nRt onto thalamic relay cells and thus form an important part of intrathalamic connectivity (Huguenard and Prince 1994b; von Krosigk et al. 1993).

Gamma-aminobutyric acid type A ($GABA_A$) receptor-mediated currents in nRt and relay nuclei are pivotal in controlling activities in this circuit. Hyperpolarizing inhibitory postsynaptic currents (IPSCs), which occur following GABA release from nRt terminals onto relay neurons, evoke rebound bursts by deinactivating low-threshold T-type calcium channels. The bursts, in turn, result in a glutamatergic reactivation of nRt neurons. Together these events are important in development of recurrent oscillatory thalamocortical rhythms (Huguenard 1999; Huguenard and Prince 1994a; von Krosigk et al. 1993), while the inhibitory connections between nRt cells serve to regulate such rhythms (Huguenard 1999; Huguenard and Prince 1994b; Ulrich and Huguenard 1997; von Krosigk et al. 1993). A detailed understanding of the structure and functional properties of $GABA_A$ receptors in nRt and neurons of relay nuclei would provide vital information on generation and control of thalamic oscillations and the processing of sensory information, improve our understanding of currently used antiepileptic drugs, and provide opportunities for rational drug design.

The $GABA_A$ receptor is a pentameric, ligand-gated Cl^- channel. Seventeen mammalian subunits have been identified. Thirteen subunits in four subfamilies are present in rat: α1–α6, β1–β3, γ1–γ3, and δ. Studies in heterologous systems have shown that subunit composition defines pharmacological and biophysical properties (MacDonald and Olsen 1994). However, analysis of subunit composition and function of native receptors has proved difficult.

In these experiments, we examined aspects of structural and functional characteristics of $GABA_A$ receptors in neurons of nRt and the ventrobasal nucleus (VB). The aim was to correlate kinetic and pharmacological properties of single channels and

* S. H. Browne and J. Kang contributed equally to this work.

Address reprint requests to J. R. Huguenard (E-mail: john.huguenard@stanford.edu).

The costs of publication of this article were defrayed in part by the payment of page charges. The article must therefore be hereby marked "*advertisement*" in accordance with 18 U.S.C. Section 1734 solely to indicate this fact.

whole cell IPSCs in individual nRt and VB neurons with data obtained using RT-PCR to examine expression of $GABA_A$ subunits in the same neurons.

$GABA_A$-receptor-mediated IPSCs recorded in nRt cells have decay time constants (τ_d) approximately threefold longer than in VB neurons (Ulrich and Huguenard 1995; Zhang et al. 1997). We tested single-channel properties that might account for this, including channel density, conductance, and open/closed times. We also examined the effects of Zn^{2+} and the benzodiazepine, clonazepam. Previous experiments on $GABA_A$ receptor-modulated responses in VB and nRt neurons have suggested that the therapeutic action of clonazepam in absence epilepsy may be related to differential effects of the drug in nRt versus thalamic relay nuclei (Gibbs et al. 1996; Hosford et al. 1997; Huguenard and Prince 1994b; Oh et al. 1995). Clonazepam decreases GABAergic output from the nRt nucleus by enhancing intranuclear recurrent inhibition but has little direct effect on $GABA_A$ responses in the VB nucleus (Huguenard and Prince 1994b). To further examine these actions at a cellular level, we investigated clonazepam's effect on monosynaptic IPSCs in nRt and VB neurons.

Knowledge of the subunit mRNAs of single nRt and VB neurons would provide information on the molecular basis for kinetic and pharmacological differences. Using a multiplex-nested strategy, we performed single-cell RT-PCR on multiple $GABA_A$ receptor subunits simultaneously, following functional characterization of each cell. We chose RT-PCR as it provides an extremely sensitive method for detecting mRNA expression of $GABA_A$ subunit isoforms present in individual cytosols. The nested design (Chiang et al. 1994; Sucher and Deitcher 1995) ensured a high level of specificity for each subunit—a necessity, given the evolutionary development of the $GABA_A$ receptor family with its extensive nucleic acid homology. By sequencing the RT-PCR products, we confirmed the specificity of the $GABA_A$ subunits detected.

METHODS

Brain slices

Brain slices containing thalamus were prepared and maintained in vitro using previously described techniques (Huguenard and Prince 1994a). Eight- to 13-day-old (P8–P13) Sprague-Dawley rats of either sex (Simonsen Breeders) were anesthetized with pentobarbital sodium (55 mg/kg ip) and decapitated. The brain was rapidly removed, and 300 μm horizontal thalamic slices were cut with a vibratome (TPI, St. Louis, MO) in a solution containing (in mM) 2.5 KCl, 1.25 NaH_2PO_4, 10 $MgSO_4$, 0.5 $CaCl_2$, 10 glucose, 26 $NaHCO_3$, and 230 sucrose. Slices containing nRt and VB were incubated in standard slice solution containing (in mM) 126 NaCl, 2.5 KCl, 1.25 NaH_2PO_4, 2 $MgCl_2$, 2 $CaCl_2$, 10 glucose, and 26 $NaHCO_3$ (pH = 7.4 when gassed with 95% O_2-5% CO_2) at room temperature (23–25°C).

Patch-clamp recordings

Slices were incubated for 1–8 h and transferred to the recording chamber (1.5 ml volume) where they were perfused with the standard slice solution at a rate of 2 ml/min at room temperature. The chamber was mounted to the fixed stage of a microscope and viewed with a ×63 objective (Zeiss Axioskop) and DIC optics and infrared illumination during recordings. Visualization of slices with a low-power objective (×2.5) allowed identification of nRt and VB. Cell-attached and outside-out patch clamp configurations (Hamill et al. 1981) were used to obtain single-channel activity from visualized neurons in VB and nRt. Recording electrodes with resistances of 4–7 MΩ were pulled from KG-33 glass capillaries (1.0 mm ID, 1.5 mm OD, Garner Glass) using a PP-83 electrode puller (Narishige, Japan). Seal resistances less than 3 GΩ were rejected. The solution for filling cell-attached patch pipettes contained (in mM) 130 KCl, 5 TEA-Cl, 2 $MgCl_2$, 10 HEPES, and 4 glucose and 2 μM GABA (pH adjusted to 7.2 with KOH). The intracellular solution for filling outside-out pipettes contained (in mM) 130 KCl, 5 EGTA, 2 $MgCl_2$, 10 HEPES, and 4 dextrose (pH adjusted to 7.2 with KOH). Single-channel activities were recorded with an Axopatch 200A amplifier (Axon Instruments, Burlingame, CA) and filtered through an eight-pole Bessel low-pass filter with 1-kHz cutoff frequency. Signals were stored both on a videotape recorder via a Neurocorder converter (Neurodata Instrument) and on computer. In outside-out patch recordings, 10 μM GABA was pressure applied (at a rate of 0.05 Hz with 20-ms, 20-kPa pulses) from a puff pipette positioned about 10 μm from the outside-out patch. The perfusion solution for Zn^{2+} experiments contained 126 NaCl, 2.5 KCl, 1.25 NaH_2PO_4, 2 $MgCl_2$, 2 $CaCl_2$, 10 glucose, and 10 HEPES (pH adjusted to 7.4 with NaOH). Dipotassium ATP (ATP), HEPES, tetra-ethylammonium chloride monohydrate (TEA), ethylene glycol-bis (*b*-aminoethyl ether)-*N*,*N*,*N*′,*N*′-tetraacetic acid (EGTA), bicuculline, and γ-aminobutyric acid (GABA) were purchased from Sigma. Other chemicals were purchased from Mallinckrodt Specialty Chemicals (Paris, KY).

Whole cell IPSC recordings and clonazepam application

Whole cell voltage-clamp recordings were obtained at a holding potential (V_{hold}) of −60 mV using an Axopatch 1A amplifier (Axon Instruments, Foster City, CA). Spontaneous IPSCs (sIPSCs) were recorded in the presence of 10 μM 6,7-dinitroquinoxaline-2,3-dione (DNQX) and 5 μM of *R*(−)-3-(2-carboxypiperazin-4-yl)-propyl-1-phosphonic acid (D-CPP) to block ionotropic glutamate receptors. The pipette solution contained (in mM) 135 CsCl, 10 EGTA, 2 $MgCl_2$, 5 N-(2,6-dimethylphenylcarbamoylmethyl)triethylammonium chloride (QX-314), and 10 HEPES, 290 mosm, pH 7.3. Signals were filtered at 2 kHz (−3 dB, 8-pole Bessel filter) and digitized. CDR and SCAN software, used to collect continuous records and detect spontaneous events, were provided by Dr. J. Dempster. The sIPSCs were characterized according to their amplitude, decay time constant and integrated area (total charge). To evaluate potential presynaptic effects of clonazepam we compared sIPSC frequencies in the absence and presence of the drug. In all instances, whole cell activity was recorded for several minutes to establish baseline values. The perfusion media was then changed to one containing the indicated concentration of the agent and after a 2- to 3-min delay to allow the drug-containing media to fill the recording chamber and the drug to diffuse into the slice, sIPSC characteristics were again evaluated. Two minutes was judged to be sufficient for replacement of media in the chamber since addition of bicuculline methiodide blocked all GABA receptor-activated currents approximately 1.5 min after addition to perfusion media (data not shown).

Single-channel data analysis

Single-channel currents were sampled every 50 μs with Fetchex and analyzed with Fetchan programs (Axon Instruments, v 6.0). A 50% threshold criterion was used to determine the durations of open and closed events. The collected open and closed intervals were binned with Pstat, and logarithmic distributions of open and closed durations were exponentially fitted using the Maximal Likelihood method. For *I-V* analysis, amplitudes were measured manually from long-duration openings. Because most outside-out patches from VB contained multiple channels, we calculated average channel open probability (P_o) using equation: $P_o = Q/(NAt)$, where Q is the integrated charge, N is the channel number in a patch, A is the amplitude of single channel current, and t the duration of integration. To obtain Q, a 1,000-ms (t) period of current following application of GABA was integrated by Clampfit. N was calculated by dividing the maximal current by A.

A

NESTED PCR WITH GENE-SPECIFIC PRIMERS

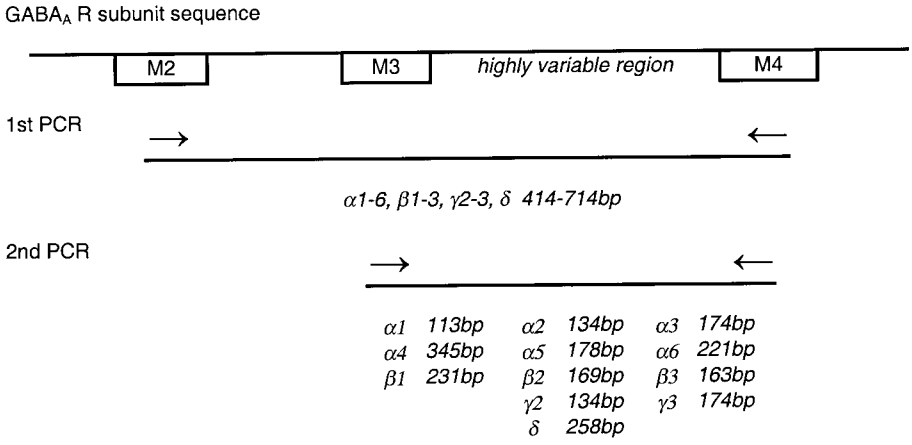

B

Outer Primers		Inner Primers	
α1	AAAGATTCCAAATAGCAGCGGAAAG	α1	GCGGTTTTGTCTCAGGCTTGAC
α1	ACGACCGTTCTGACCATGACAACCT	α1	CTCCTACAGCAACCAGCTATACCC
α2	AAAAGTACCAAACAGAACCGGGAAC	α2	GCTTCTTGTTTGGTTCTGGAGTAG
α2	GACAATGACCACATTAAGCATCAGT	α2	AAGAGAAAGGCTCCGTCATG
α3	GAATATGGCAAAGAGCACAGGGAAG	α3	AGGTCTTGGTCTCAGCAGGA
α3	ACCACTGTTCTCACCATGACCACCT	α3	ACAAGCACCACCTTCAACATAG
α4	AAATGCCCCAAATGTGACTGGAAAG	α4	TTGTGCCAGATCCAGAAGGTGGTG
α4	ACCACAGTCCTCACGATGACCACCC	α4	GATGTCAACAGCAGAACTGAGGTG
α5	GAAAGTGCCAAACAAAATGGGGAAC	α5	GAAGTCTTCTCCTCAGATGCTCT
α5	ACCACAGTGCTCACCATCACAACCC	α5	GCCTTGGAAGCAGCTAAAATC
α6	GAATCCTGCAAATGCTACTGGGAAG	α6	GTACACAAGGTTGAATCCTG
α6	ACCACGGTTTTAACCATGACCACCT	α6	CACTCTGACTCCAAGTACCATCTG
β1	AAAAAGGGAAAATGTOATGGGGAAG	β1	TCACGGCTGCTCAGTGGTTT
β1	ACCACGGTGCTGACCATGACAACCA	β1	CCCTCAGAAAAAAGGAGCGA
β2	GAAGAAGGAAAACACCACAGGGAAC	β2	CTAGGCAACCCAGCTTTCCGATAC
β2	ACAACTGTCCTGACGATGACCACAA	β2	GCCTGGATGTCAACAAGATGGACC
β3	GAAGAGAGAAAAGGTGAATGGAAAC	β3	GATGCTTCTGTCTCCCATGTAC
β3	ACCACCGTGCTCACCATGACAACCA	β3	CCTACTAGCACCGATGGATGTT
γ2	GAACAAGCAGAAGGCGGTAGGGAAG	γ2	TCTCTTGAAGGTGGGTGGCA
γ2	ACGACTGTCCTGACGATGACCACTC	γ2	CGGAAACCAAGCAAGGAT
γ3	GAACAGCAGGAAGGACGTTGGGAAG	γ3	AACTCCTGCCAGTACATGGAATTG
γ3	ACCACGGTGCTAACCATGACCACAC	γ3	GCTGTCGAAAGCCAACCATCAG
δ	GACTGCTGCAAAGGCTGCCGGGAAC	δ	TTGAGTCTGGAACGGATGCCTC
δ	ACCACTGTGCTGACAATGACCACAC	δ	CCCACTTCAATGCTGACTACAGG

FIG. 1. *A*: nested PCR rational and product sizes. The 1st PCR amplification took place across transmembrane regions M2–M4, represented as closed boxes in diagram. Given the considerable heterogeneity between the subunits, even within the families, it was not possible to use degenerate primers and equally amplify all the subunits. Thus a primer pair set was developed for each subunit. The primers were tested carefully, optimization (data not shown) revealed that all outer primers performed optimally at 55° and 3 mM $MgCl_2$, allowing pursuit of simultaneous analysis. DNA products from the 1st-round PCR were used, after dilution, as templates for a further amplification reaction. This second PCR analysis amplified across the highly variable region M3–M4, providing sequences entirely unique to each of the 13 subunits. The 2nd-round fragment was thus internal to the 1st-round fragment providing an additional measure of internal control. The lengths of the expected fragments are listed. Second-round PCR products were nucleotide sequenced to confirm accuracy. *B*: sequences of $GABA_A$ primers; the 1st sequence of each pair is the antisense primer, the 2nd is the sense primer. Outer primers were used in the 1st-round amplification and inner primers in the 2nd-round amplification. Primers used in this experiment were designed using MacVector software 5.0.

RNA harvest and reverse transcription with random primers

NRt and VB neurons were initially identified by anatomical position in the thalamic slice and morphological appearance under Nomarski optics. All cells from which cytosols were harvested were characterized electrophysologically prior to PCR subunit analysis and had characteristic nucleus-specific IPSCs (Huntsman and Huguenard 2000)—i.e., sIPSCs in VB neurons occurred at a higher frequency and had more rapid decay kinetics than those in nRt cells.

Positive pressure on the silanized patch pipette as it was lowered into the preparation prevented contamination of the samples (Chiang 1998). After whole cell voltage-clamp recordings, negative pressure was applied to the pipette and the contents of the cell aspirated into a silanized micropipette; successful harvest was monitored via microscopy. The cytosol was expelled into an RNase-free silanized microcentrifuge tube containing 10 μl of reverse transcription reagents: 0.5 mM each deoxynucleotide (dNTP; Boehringer Mannheim, Indianapolis, IN), 5 μM random hexamer oligonucleotide (New England Biolabs, Beverly, MA), 10 U/μl reverse transcriptase (Superscript II, Gibco BRL, Grand Island, NY), 2 U/μl RNase inhibitor (RNasin, Promega, Madison, WI), 10 mM dithiothreitol (DTT), and 50 mM Tris-HCl (pH, 8.3). The mixture was incubated for 15 min at room temperature followed by 1 h at 37°C. The reaction was terminated by 5 μg yeast tRNA (Sigma, St. Louis, MO), 0.3 M sodium acetate (pH, 7.0) and 250 μl ethanol, and the mixture stored at −20°C. Prior to PCR, the single cell cDNA template was recovered by centrifugation, washed with 70% aqueous ethanol, and resuspended in 3 μl RNase-free H_2O, i.e., Millipore filtrated water (Water Purification Systems, Bedford, MA) autoclaved for 45 min in baked glassware.

PCR amplification

Multiplex PCR with a nested design strategy was performed using two approaches: in single cytosol experiments, an individual cell precipitate was used as cDNA template for PCR and in the combined cytosol experiment, 10 nRt single cytosol and 10 VB single cytosol cDNA precipitates were combined according to cell type to produce two templates for PCR. In the first round of PCR, outer primers for each individual $GABA_A$ subunit tested were employed simultaneously (for primer sequences see Fig. 1*B*). In the single-cytosol experiments, primer sets for α1, -2, -3, and -5 and γ2 subunits were used and in the combined single cytosol experiment, 12 primer sets were used in the first round of PCR. The primer pair sets used for γ1 subunit performed inadequately and thus have been excluded from this analysis.

The PCR mixture consisted of 50 mM Tris-HCl (pH 8.3), 500 μg/ml bovine serum albumin (BSA), 200 μM dNTP, 0.5 μM of each primer pair, 2 U *Taq* polymerase (Perkin Elmer Cetus, Foster City, CA) + *Taq* Start antibody(1:1) (Clontech, Palo Alto, CA), 3 mM $MgCl_2$ and template to a total volume of 10 μl. The PCR conditions were 2 min at 94°, 30 cycles with an annealing temperature of 55°C and 2 min at 72°C (i.e., temp D = 94, A = 55, E = 72; time instantaneous, instantaneous, 0.15; slope, 2.0) performed on Rapid Thermocycler Model No. 1002 (Idaho Technology).

The resulting multiplex amplification product was then diluted into 80–100 μl milliQ H_2O. One to 3 μl of the diluted first round PCR product were then used as template for a second round. In this portion of the experiment, parallel PCRs containing one pair of gene-specific nested primers per reaction were performed. The PCR mixture and PCR conditions were the same as in the first round. Positive and negative control samples were run simultaneously with the $GABA_A$ subunits through the first and second rounds of PCR. Positive controls included reactions with adult rat brain of cDNA (1 ng/μl) and single-cell template with primers for glyceraldehyde phosphate dehydrogenase (GAPDH). Negative control reactions included template of RNase free H_2O and template from mock patch-pipette insertion into preparation without aspiration of a cytosol to monitor harvest contamination.

Gene expression was detected by agarose gel electrophoresis (Metaphor Agarose 3%, FMC, Rockland, ME), stained with ethidium bromide, of the entire product from the second round PCR run in parallel with known molecular weight markers (Lambda DNA restricted with *Bgl*II; pBR322 plasmid DNA restricted with *Hpa*II). Expected sizes of the amplified $GABA_A$ subunit fragments were calculated from the published sequences (see Fig. 1*A*). To confirm the identity of the amplified fragments, each product was nucleotide sequenced.

Sequencing protocol

PCR product from each subunit nested primer pair set was gel purified and prepared for sequencing using the PE Applied Biosystems Terminator Ready Reaction Mix (Perkin Elmer Cetus): 8.0 μl terminator ready reaction mix, approximately 85 ng PCR product, 3.2 pmol of 5′ nested primer with deionized water to volume of 20 μl. After a brief spin, the Ericomp TwinBlock System thermal cycler Model No. 1002 was used for the following reaction: 96°C for 20 s, repeat for 25 cycles; 96°C for 10 s, 50°C for 5 s, 60°C for 4 min, 20°C for 30 min. Extension product was purified by phenol-chloroform extraction and ethanol precipitation. Air-dried DNA pellet was sent to the Protein and Nucleic Acid (PAN) Facility of Stanford University Medical Center for sequencing.

Statistical analysis

All results are provided as means ± SE, and statistical significance assessed with a two-sided *t*-test, except in the case of the effects of clonazepam on sIPSC decay, in which an ANOVA with post hoc Tukey test was used.

RESULTS

Single-channel properties of $GABA_A$ receptors in cell-attached patches from nRt and VB neurons

The single-channel properties of $GABA_A$ receptors in nRt and VB neurons were examined using the cell-attached patch configuration. GABA (2 μM) was added to the pipette solution. $GABA_A$ channel activities were seen in 8 of 10 patches from nRt neurons and in 5 of 5 patches from VB neurons. Channel density was higher for VB (2.8 ± 0.4/patch, $n = 5$ patches) versus nRt neurons (0.9 ± 0.2/patch, $n = 10$ patches). The observed channels were $GABA_A$ receptors because no openings were observed in patches obtained with pipettes filled with solution containing 20 μM bicuculline ($n = 5$ patches) and extrapolated reversal potentials (−50 to −60 mV) were close to the calculated E_{Cl} (Fig. 2*B*). The channels from nRt patches showed longer openings than those from VB patches (Fig. 2*A*). Both nRt and VB channels showed a major conductance (Fig. 2*A*, o) and a subconductance (Fig. 2*A*, sub) state. The major conductances were 16 ± 0.5 pS ($n = 5$ patches) and 17 ± 1.7 pS ($n = 5$ patches) for nRt and VB channels, respectively (Fig. 2*B*). Neither the single-channel conductance nor the extrapolated reversal potential showed significant differences between nRt and VB channels (Fig. 2*B*). Kinetic analysis indicated that open time distributions for nRt channels were longer than for VB channels (Fig. 2*C*). Mean open time for nRt channels was 14.6 ± 2.5 ms ($n = 5$ patches), which was significantly longer than that for VB channels (3.8 ± 0.7 ms, $n = 5$ patches; $P < 0.01$).

Single-channel properties of $GABA_A$ receptors in outside-out patches from nRt and VB neurons

Outside-out patches were directly excised from somata of nRt or VB neurons in slices. When patches were held at −80

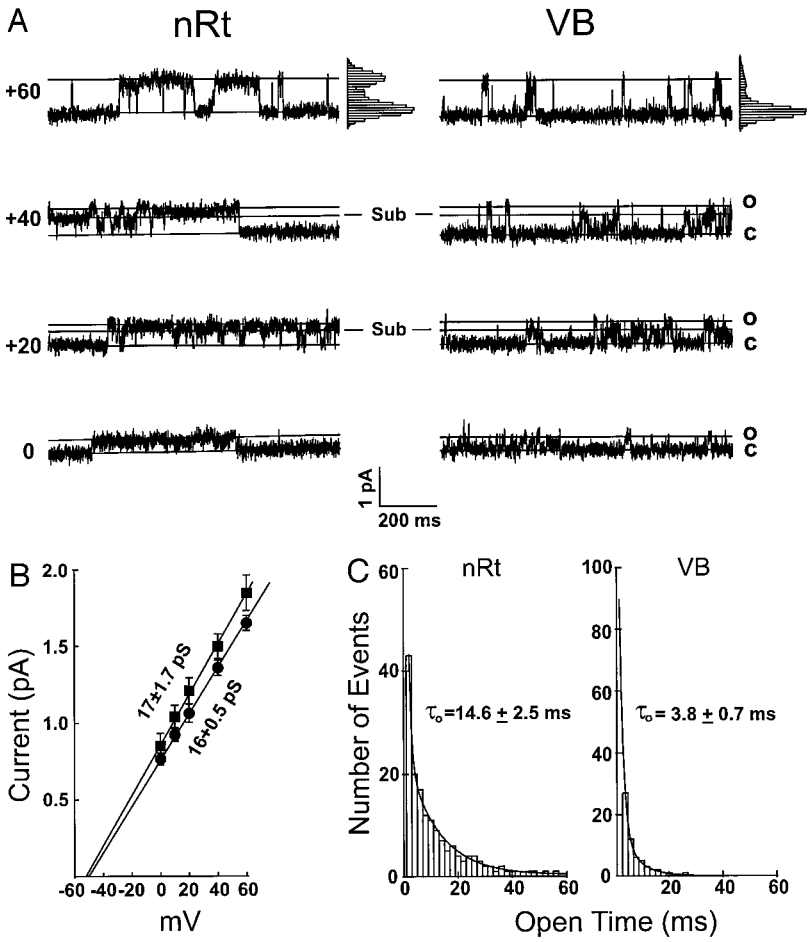

FIG. 2. $GABA_A$ channels in cell-attached patches. *A*: channel activities recorded from representative reticular nucleus (nRt) and ventrobasal complex (VB) neurons at different membrane potentials. The numbers at the *left* of traces are potentials across the patch membrane. The resting membrane potential was assumed to be −65 mV according to whole cell recordings in these cells (Cox et al. 1995). The upward direction indicates outward current (influx of Cl^-). Solid lines indicate the closed state (c), and dashed lines indicate the major open state (o) and the subconductance state (sub). The graph at the *right* of the top trace is an all-points histogram for the trace. *B*: current vs. voltage relationships (*I-V*) for $GABA_A$ channels in nRt (■) and VB (●) neurons. Numbers indicate mean values of the slope conductance for nRt and VB channels ($n = 5$ patches for each). *C*: kinetics of $GABA_A$ channels in nRt and VB neurons. Graphs are open time distributions for the nRt and VB channels presented in *A*. Numbers in graphs are means ± SE ($n = 5$ patches for each) of mean open times (t_o). Membrane potential was +15 mV.

mV, very few channel openings were observed in the absence of GABA (Fig. 3, *Aa* and *Ba*, before ↓). When 10 μM GABA was applied to the tip of patch pipettes, frequent channel openings were observed (Fig. 3, *Aa* and *Ba*, after ↓). In agreement with the results from cell-attached recordings (*above*), channel numbers in outside-out patches from VB neurons (7.17 ± 1.80/patch, $n = 6$ patches) were larger than those from nRt neurons (2.14 ± 0.14/patch, $n = 7$ patches). As

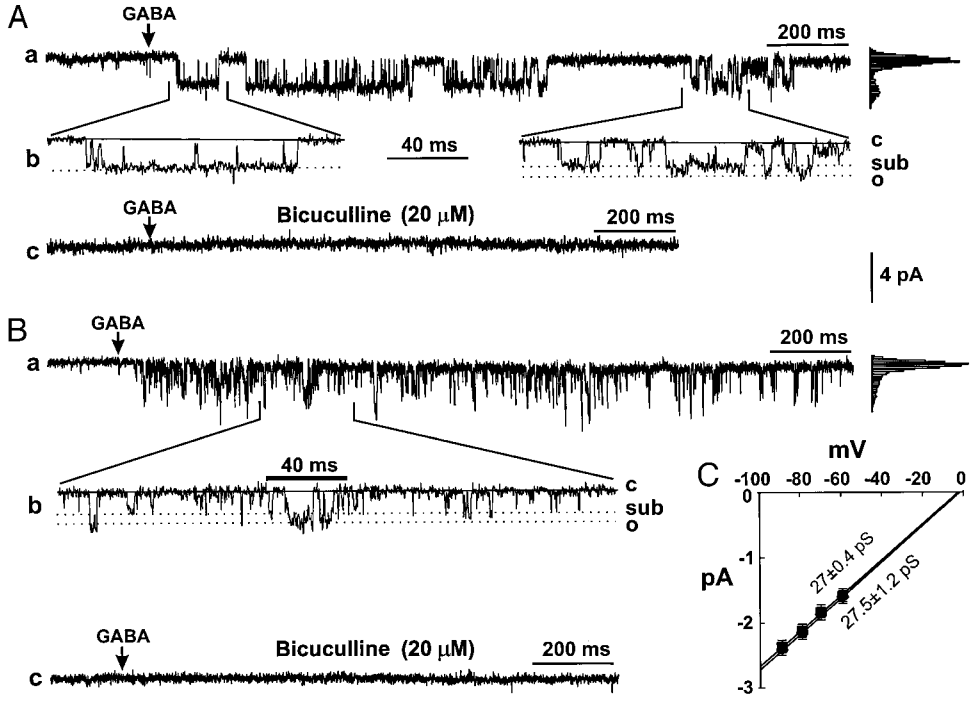

FIG. 3. Single-channel properties of $GABA_A$ receptors in outside-out patches. Outside-out patch recordings were obtained with symmetric Cl^- (140/140 mM) at a holding potential of −80 mV. GABA (10 μM) was applied at the time indicated by an arrow. The graph at the *right* of traces (*a*) is an all-points amplitude histogram. The nRt channels showed a longer open duration (*A, a* and *b*) than VB channels (*B, a* and *b*). Both nRt and VB channels were inhibited by 20 μM bicuculline (*c*). *I-V* curves showed a similar conductance (~27 pS) and a similar reversal potential (~0 mV) for nRt (●) and VB (■) channels (*C*).

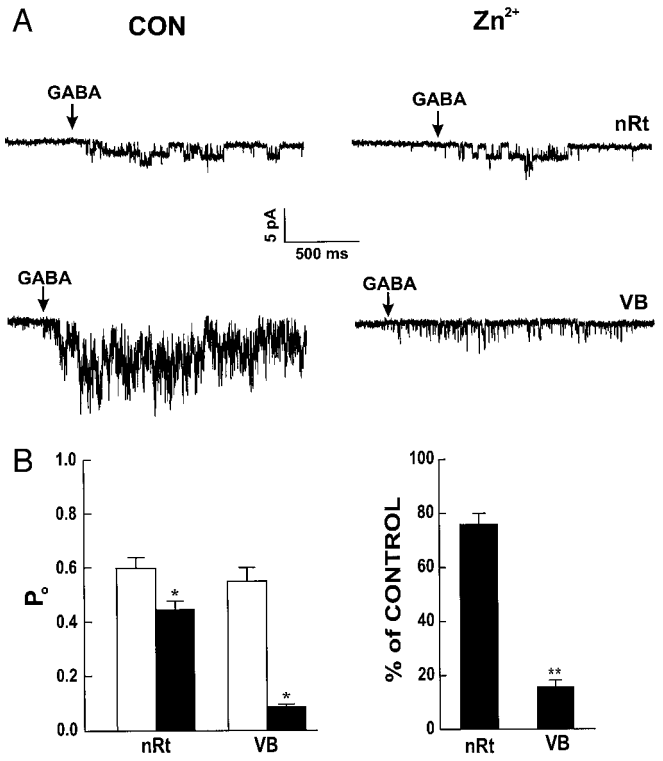

FIG. 4. Inhibition of nRt and VB $GABA_A$ channels by Zn^{2+}. Outside-out patch recordings were obtained as described in Fig. 2. *A*: representative responses of nRt (*top*) and VB (*bottom*) channels to 10 μM GABA before (CON) and after (Zn^{2+}) perfusing the solution with added 100 μM Zn^{2+}. *B*: bar graphs showing effects of 100 μM Zn^{2+} on average open probability (P_o) of nRt and VB channels. *Left*: P_o for channels in the absence (□) or presence (■) of Zn^{2+}. *Right*: percentage of control P_o for Zn^{2+}-inhibited nRt and VB channels. *, $P < 0.01$ compared with control. **, $P < 0.01$ compared with nRt channels. $n = 5$ and 8 patches for VB and nRt, respectively.

expected, nRt channels showed longer openings (Fig. 3*A*, *a* and *b*) than VB channels (Fig. 3*B*, *a* and *b*). All point histograms showed a well-defined peak associated with the open state for the nRt channels (Fig. 3*Aa*, graph at *right*) but not for VB channels (Fig. 3*Ba*, graph at *right*), likely because system filtering attenuated the shorter VB openings. Both nRt and VB channels were sensitive to 20 μM bicuculline (Fig. 3, *Ac* and *Bc*) and showed a major conductance and a subconductance state (Fig. 3, *Ab* and *Bb*, o and sub). The major conductance was 27.0 ± 0.4 pS ($n = 6$ patches) and 27.5 ± 1.2 pS ($n = 2$ patches) for nRt and VB channels, respectively (Fig. 3*C*).

Interestingly, it has previously been reported that miniature IPSC (mIPSC) amplitude is comparable in nRt and VB cell recordings (Ulrich and Huguenard 1996). The threefold higher $GABA_A$ channel density in somatic VB membranes, obtained with both outside-out and cell-attached patches, suggests that synaptic channel counts are unrelated to somatic channel density.

Sensitivity of nRt and VB channels to Zn^{2+}

We further tested pharmacological properties of nRt and VB channels by perfusing outside-out patches with a solution containing 100 μM Zn^{2+}. The activity of nRt channels was slightly inhibited (Fig. 4*A*, *top*), while VB channel openings were markedly attenuated by Zn^{2+} (Fig. 4*A*, *bottom*). To quantitatively analyze Zn^{2+} effects, we calculated channel open probability (P_o). Because most patches from VB neurons contained multiple channels, a value of averaged P_o was obtained by integration (see METHODS). In control recordings, nRt and VB channels showed similar average P_o (0.60 ± 0.04, $n =$ 8 patches and 0.55 ± 0.05, $n = 5$ patches, respectively) after exposure to GABA (Fig. 4*B*, *left*). When a solution containing 100 μM Zn^{2+} was perfused, P_o for VB channels was reduced to 0.09 ± 0.01 ($n = 5$ patches) while P_o for nRt channels decreased to 0.45 ± 0.03 ($n = 8$ patches). Reduction of VB channel activity by 100 μM Zn^{2+} (84%) was significantly larger than that for nRt channel activity (24%) (Fig. 4*B*, *right*, $P < 0.01$). This result indicates that VB $GABA_A$ receptor channels are more sensitive to Zn^{2+} than nRt channels.

Spontaneous IPSCs in nRt and VB cells and the effect of clonazepam

In the neurons of the present experiments, the IPSC decay was reasonably described by a single exponential decay. As previously reported (Zhang et al. 1997), sIPSC decay time constants were slower for nRt (45.2 ± 12.1; $n = 9$) than for VB neurons (17.3 ± 5.3 ms; $n = 8$). The 10–90% rise times were 1.7 ± 0.5 ms for nRt and 1.8 ± 0.5 ms for VB neurons. Typical sIPSCs are shown in Fig. 5. The frequency of sIPSCs was 1.2 ± 1.0 Hz in nRt neurons and 5.6 ± 5.0 Hz in VB cells. sIPSCs were completely blocked by 20 μM bicuculline methiodide applied to the bath (data not shown).

We studied the effect of nM concentrations of clonazepam (CZP) on sIPSCs from 17 nRt and 15 VB neurons. Figure 6*A* shows the effect of 50 nM clonazepam on sIPSCs from nRt and VB. The traces are averaged spontaneous events ($n > 20$)

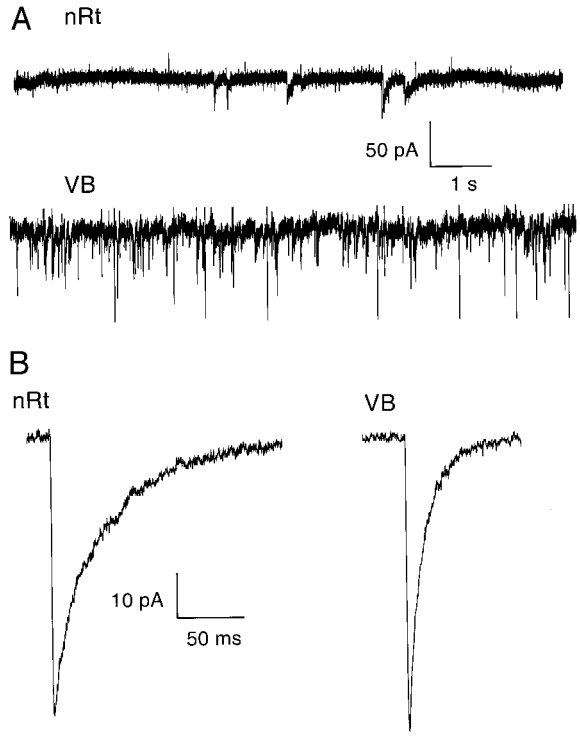

FIG. 5. Spontaneous inhibitory postsynaptic currents (IPSCs) from thalamic neurons of the nRt and the VB. *A*: continuous data traces showing spontaneous (sIPSCs) in VB and nRt. *B*: averaged sIPSCs from single neurons in nRt and VB. Recording temperature was 30°C; $V_{hold} = -60$ mV, estimated $E_{Cl} = 0$ mV.

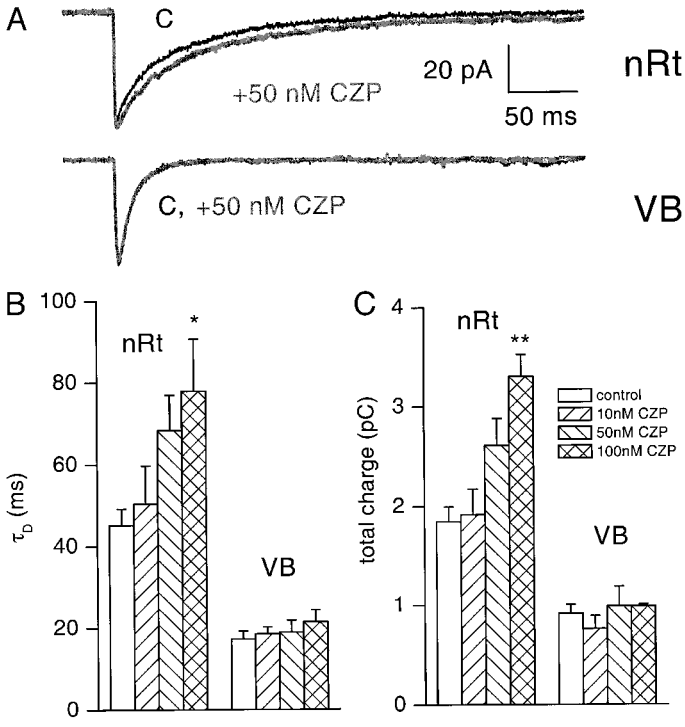

FIG. 6. The effect of clonazepam on sIPSCs in thalamic neurons. *A*: clonazepam (CZP) increases the τ_d and total charge of the sIPSC in nRt but not VB. *B* and *C*: effects of increasing concentrations of clonazepam on τ_d and charge of sIPSCs in nRt and VB. *, $P < 0.05$; **, $P < 0.05$ (ANOVA with post host Tukey test).

recorded before and after the addition of CZP. At this concentration, CZP selectively prolonged the time course of sIPSCs in nRt.

These effects in nRt were concentration dependent, as shown in Fig. 6, *B* and *C*, for 10–100 nM CZP. Results are summarized in Table 1. In the presence of 100 nM CZP, τ_d in nRt increased 76% from 44.3 to 77.9 ms ($P < 0.01$); however, in VB the increase was insignificant, from a baseline value of 15.6 to 21.4 ms (37%; $P > 0.05$). In the reticular nucleus, all cells ($n = 8$) were influenced by clonazepam, and the integrated area of sIPSCs increased by 79%, from 1.85 pC in control to 3.31 pC after CZP ($P < 0.01$), while in VB, the total charge was not affected (0.92 and 0.99 pC in control and CZP, respectively; $P > 0.05$; Fig. 6*C*). Clonazepam had no effect on amplitude of sIPCSs at either site (data not shown).

TABLE 1. *The decay time constant (τ_D) and total charge of sIPSCs from nRt and VB in control and with various concentrations of clonazepam*

	nRt		VB	
	τ_D, ms	Charge, pC	τ_D, ms	Charge, pC
Control	45.2 ± 4.0	1.85 ± 0.15	17.3 ± 1.9	0.92 ± 0.09
Clonazepam				
10 nM	50.4 ± 9.3	1.92 ± 0.26	18.5 ± 1.7	0.77 ± 0.13
50 nM	68.3 ± 8.6	2.61 ± 0.27	18.9 ± 2.9	0.99 ± 0.20
100 nM	77.9 ± 12.8*	3.31 ± 0.22**	21.4 ± 2.9	0.99 ± 0.02

Values are means ± SD. nRt, reticular nucleus; VB, ventrobasal complex; sIPSCs, spontaneous inhibitory postsynaptic currents. * $P < 0.05$; ** $P < 0.01$.

In nRt cells, the effects of 100 nM CZP on τ_d and total charge were statistically significant ($P < 0.05$ and $P < 0.01$, respectively), whereas in VB, there was a small, statistically insignificant increase in τ_d (Fig. 6*B*). The frequency of sIPSCs was not altered significantly in either nucleus by clonazepam. Control sIPSC amplitudes in nRt and VB neurons were not significantly different, and at these concentrations, clonazepam had no significant effect on amplitude.

Expression of $GABA_A$ subunit mRNA

To elucidate the molecular basis for the differences observed, we used multiplex nested single-cell RT-PCR. We found it was not possible to use degenerate primers and amplify each subunit equivalently in our multiplex system. This was due to the heterogeneity of nucleotides observed, even within families. For this reason, individual primer pair sets were used for each subunit (see Fig. 1*A*). Primer pairs were carefully and extensively tested; all first round primers were optimized to the same conditions allowing simultaneous amplification (data not shown). Nested primers were designed to cross the highly variable transmembrane region (see Fig. 1*A*). Despite this, it was necessary to amplify smaller fragments than initially expected to ensure specific subunit amplification.

We performed two experiments, the first on single cytosols looking at 5 $GABA_A$ subunits simultaneously and the second on samples combining 10 cytosols of each cell type looking at 12 $GABA_A$ subunits. Initially, PCR amplification was performed on single-cell cytosols. Cells without PCR product were rejected, 11 single cells were analyzed: 7 VB cells and 4 nRt cells. Both positive and negative controls were performed through both rounds of PCR (see experimental procedures). Table 2 shows expression of α1–α3 and -5 and γ2 in these cells. Expression of α subunits was markedly different between VB and nRt cells. In general, VB cells expressed more α subunits. All seven VB cells expressed α1, and some expressed all four α subunits. The only α subunits observed in nRt cells were α3 and α5 (1 each in 1 of 4 cells). γ2 signal was detected in both types of cells. Figure 7 provides an example of α1 signals detected in 4/4 VB and 0/3 nRt cells and γ2 detected in all cells.

Cell-to-cell differences in signal detection may reflect heterogeneity in levels of single-cell gene expression. Signal detection is also affected by the sensitivity of the assay and the

TABLE 2. *Expression of $GABA_A$ subunits α1–α3 and -5 and γ2 in single VB and nRt cells*

	α1	α2	α3	α5	γ2
nRt	−	−	−	−	+
nRt	−	−	−	−	+
nRt	−	−	+	−	+
nRt	−	−	−	+	−
VB	+	+	−	+	+
VB	+	+	+	+	−
VB	+	+	−	+	+
VB	+	+	−	−	+
VB	+	+	−	+	+
VB	+	+	+	+	−
VB	+	−	+	+	−

−, no apparent PCR product by ethidium bromide stained gel electrophoresis; +, appropriately sized PCR product.

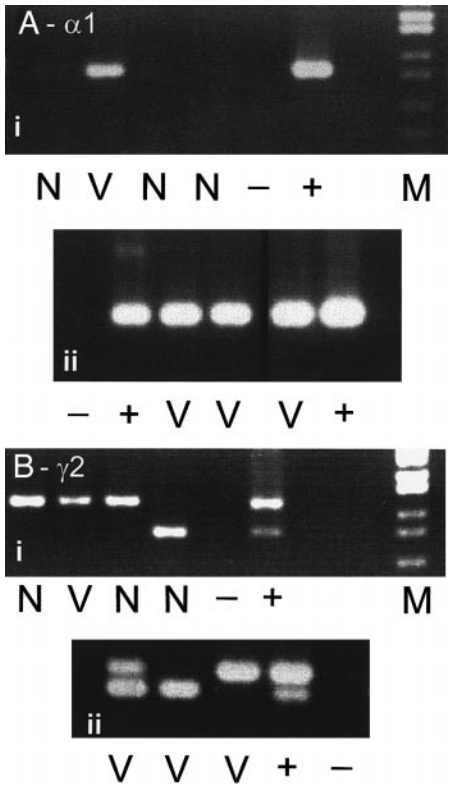

FIG. 7. PCR products from single nRt and VB neurons run on ethidium bromide-stained metaphore agarose gel showing examples of expression of *A, i* and *ii*: α1 subunit, and *B, i ii*: γ2 subunit in 3 single nRt and 4 single VB neurons. Lanes labeled N are nRt single cell signals, Lanes V are single VB cell signals, −, Rnase-free H_2O as template, +, total brain cDNA as template, and lanes labeled M indicate reference pBR322 plasmid DNA restricted with *Hpa*II. Signals in *Aii* are from same agarose gel as are those in *Bii*. Note that the γ2 lanes show 2 transcripts corresponding to the short and long splice variants.

adequacy of the cytosol harvest. As regards sensitivity, we estimated, using serial dilution of template, that under optimal multiplex RT-PCR assay conditions for 6 and 12 primers, approximately 30 molecules of RNA could be detected (data not shown). In other words, to detect a signal, at least 30 molecules of mRNA had to be present in the cytosol harvested.

To avoid limits associated with unequal harvest of cytosols from individual cells, we combined and analyzed 10 cytosols of each type. By combining cytosols the likelihood of missing contributing portions of cytosol was minimized. Further, the increased template concentration allowed simultaneous use of 12 subunit primer pairs. Table 3 shows expression of $GABA_A$ subunits in 10 pooled VB and 10 nRt cells. Figures 8 and 9 show the corresponding ethidium-bromide-stained metaphor agarose gels. There were marked differences between VB and nRt cells in the expression of α subunit subtypes in the combined cytosol experiment, a finding similar to that in single

TABLE 3. *Expression of $GABA_AR$ subunits in neurons of nRt and VB, derived from pooled cytosols*

	α1	α2	α3	α4	α5	α6	β1	β2	β3	γ2	γ3	δ
nRt	−	−	+	−	+	−	−	−	−	+	+	+
VB	+	+	+	−	+	−	+	+	+	+	+	+

Gel bands were evaluated as present (+) or absent (−).

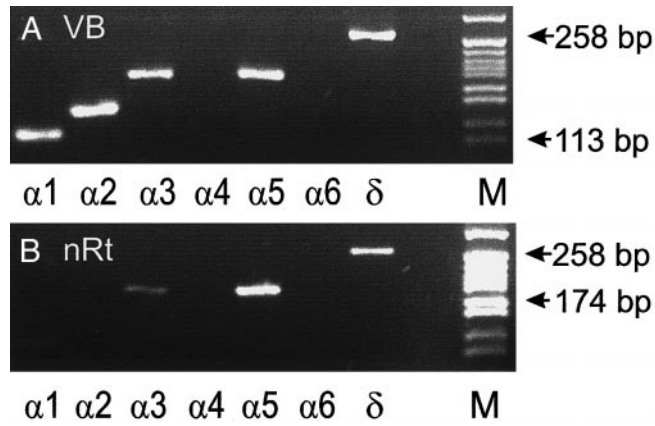

FIG. 8. PCR products from 10 VB and 10 nRt neurons run on an ethidium-bromide-stained metaphore agarose gel showing α and δ subunits signals detected after the 2nd round of PCR amplification. *A*: VB. *B*: nRt. Primers used as follows: α1, lane 1; α2, lane 2; α3, lane 3; α4, lane 4; α5, lane 5; α6, lane 6; δ, lane 7. Included for reference is pBR322 plasmid DNA restricted with *Hpa*II.

cells. The nRt cells analyzed appeared to express only α3 and -5 subtypes, whereas VB neurons expressed α1–α3 and -5. As expected, alpha 6 was not seen in either cell group (McKernan and Whiting 1996). The α4 subunit was not found in either cell type, although, it was present in all the positive controls. γ2 (both splice variants) and γ3 were observed in both nRt and VB cells (Fig. 9*B*). No obvious signal for any β subunit was found in nRt, while all three β subunits were found in VB cells. Signal for the delta subunit was also found in both cell types.

Summary of results

In this study, we provide evidence that kinetic and pharmacological differences in $GABA_A$ receptors in single thalamic

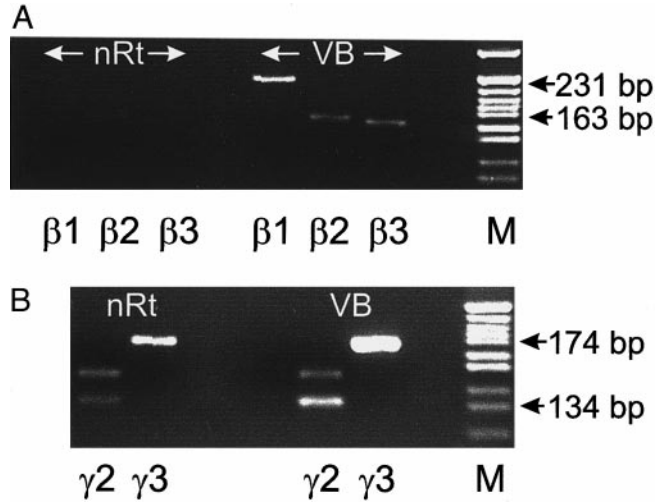

FIG. 9. PCR product from 10 VB and 10 nRt neurons run on ethidium-bromide-stained metaphore agarose gel showing β and γ subunit signals detected following the 2nd round of PCR amplification. *A*: β1–β3 transcripts. Lanes 1–3 are nRt cell templates and lanes 4–6 are VB cell templates. Included for reference is pBR322 plasmid DNA restricted with *Hpa*II (M). Very weak bands were occasionally observed for β subunits in nRt cells, but for the purposes of our present analysis, these were deemed negative. *B*: γ2 and γ3 transcripts. Lanes 1 and 2 are nRt cell templates and lanes 3 and 4 are VB cell templates. Included for reference is pBR322 plasmid DNA restricted with *Hpa*II (M).

neurons are associated with heterogeneity of $GABA_A$ subunit expression. VB cells had shorter single-channel open times than nRt cells, and VB single-channel activity was significantly reduced by 100 μM Zn^{2+}. Whereas nRt cells showed a significant increase in IPSC τ_d when exposed to nanomolar clonazepam, VB cells did not. VB cells studied expressed α1–α3 and -5, β1–β3, γ2 and γ3, and δ, while nRt cells expressed α3 and -5, γ2 and -3, and δ $GABA_A$ receptor subunits.

DISCUSSION

Distinct single-channel properties of $GABA_A$ receptors ($GABA_A$Rs) in nRt and VB cells underlie differences in IPSCs

Openings of nRt $GABA_A$ channels, recorded in both outside-out and cell-attached patches, were about threefold longer than for VB channels. Therefore the previously reported difference in sIPSC duration between nRt and VB neurons (Zhang et al. 1997) can largely be explained by differences in single-channel kinetics. Differences in rise times have not been observed, which suggests that the on-rate for GABA is not different for the two $GABA_A$ channel types. Further, differences in single-channel amplitudes or subconductance states were not observed. Channel density was much higher in VB cells, which is in agreement with the differences in evoked IPSC amplitude in the two cell types (Zhang et al. 1997).

$GABA_A$R subunit mRNA expression in VB vs. nRt cells

Our results indicate that the major difference in subunit expression in neurons of VB versus nRt is in the α and β subunits. VB cells expressed α1–α3 and -5 and β1–β3, while nRt cells studied expressed α3 and -5. Neurons of both structures expressed γ2 and -3 and δ. Our findings are relevant for rat brain aged 8–12 days (i.e., P8–P12). The $GABA_A$ receptor in the thalamus reaches a mature configuration by the end of the third postnatal week (Bentivoglio et al. 1990). Few prior studies of postnatal $GABA_A$ subunit mRNA distribution in the rat brain have distinguished between nRt and VB nuclei; rather, results have focused on expression in the entire thalamus or diencephalon (Laurie et al. 1992; Poulter et al. 1993). Because of this, we have compared our results to those in both immature and adult rats.

Our findings of α1–α3 and -5 subunits in VB cells are consistent with literature for rats of this age (Fritschy et al. 1994; Laurie et al. 1992). α3 subunits are also known to be expressed in nRt (Fritschy et al. 1994; Laurie et al. 1992; Wisden et al. 1992). γ2 subunits (both splice variants) have been detected in both VB and nRt in immature (Laurie et al. 1992; Poulter et al. 1993) as well as in adult animals (Fritschy et al. 1994; Wisden et al. 1992). Similarly, γ3 is present in thalamus in immature animals (Laurie et al. 1992; Poulter et al. 1993) and in both nuclei in adults (Wisden et al. 1992). The δ subunit, which we found in both cell types, has been detected in thalamic nuclei from p12 (Laurie et al. 1992) but not consistently (Poulter et al. 1993). In adult animals, δ is reportedly present in nRt and VB (Fritschy and Mohler 1995) or in ventroposterior medial nucleus only (Wisden et al. 1992).

Interestingly, we did not observe a signal for α4 in either cell type, although strong signals were found in all positive controls. This is in contrast to previous in situ hybridization and immunostaining results (Fritschy and Mohler 1995; Laurie et al. 1992; Pirker et al. 2000) and might be due to the developmentally immature animals studied or could be a false negative result.

All three β isoforms were present in VB cells. We did not detect β isoforms in nRt, a finding consistent with previous immunohistochemical and in situ hybridization studies which failed to detect β2/β3 protein or mRNA in nRt (Fritschy and Mohler 1995; Fritschy et al. 1994; Spreafico et al. 1993). However, a recent study using specific antibodies demonstrated β1- and β3-like immunoreactivity in neuropil and neuronal processes of nRt (Pirker et al. 2000). Similarly, an in situ hybridization study of $GABA_A$ receptors in monkey thalamus demonstrated low but detectable levels of β1 and β3 subunits in the reticular nucleus (Huntsman et al. 1996). Recently, Huntsman et al. (1999) found that mice devoid of β3 have severely disrupted intra-nRt inhibition and display thalamic hypersynchrony, which strongly implicates a role for β3 in nRt function. The results of the latter three studies suggest that the very low (or in this case, even below the threshold for detection) levels of β subunit mRNA (Wisden et al. 1992; this study) are sufficient for expression of functionally relevant levels β subunit protein. Alternatively, nRt neurons may possess functional $GABA_A$ receptors with no β subunits. Fritschy et al. (1992) and Fritschy and Mohler (1995) suggested that a minor $GABA_A$ receptor subtype, composed of $\alpha\gamma$ subunits, exists in rat brain. In recombinant systems α, β and γ subunits are generally considered necessary for fully functional $GABA_A$ receptors (Pritchett et al. 1989). However, there are multiple examples of functional $GABA_A$ receptors composed of α, γ subunit combinations that exhibit GABA-gated chloride channels modulated by benzodiazepine site ligands (Granja et al. 1997; Im et al. 1993; Knoflach et al. 1996; Wong et al. 1992, in HEK cells; Angelotti et al. 1993, in L929 fibroblasts). Such receptors have a main-conductance level of 30pS (Verdoorn et al. 1990), similar to those in neuronal $GABA_A$ receptor channels (Angelotti and Macdonald 1993), and could potentially subserve $GABA_A$ receptor function in nRt.

α subunits appear pivotal in the differential kinetics of $GABA_A$Rs in VB and nRt cells

Consideration of the kinetic analysis of IPSCs, together with subunit expression patterns, suggests that the significant differences in decay time constants in nRt and VB cells may correlate with differences in the α or β subunits. Considerable work from recombinant systems suggests the structural determinant of $GABA_A$ receptor channel activation/deactivation kinetics resides with the α subunit (Gingrich et al. 1995; Lavoie et al. 1997; Tia et al. 1996; Verdoorn 1994). Gingrich et al. (1995) indicated that substitution of α3 for α1 in a recombinant receptor slowed deactivation threefold. Verdoorn (1994) also found that the decay time courses of currents mediated by receptors containing α3 were slower than those containing α1, or, both α1 and α3. Given such work in recombinant systems, it is likely that the slower τ_d in nRt versus VB neurons relates to the presence of α1 in VB and not nRt cells, and from our data and that of others (Fritschy et al. 1994; Laurie et al. 1992), the incorporation of an α3 subunit in nRt neuronal $GABA_A$ receptors.

Pharmacological differences in $GABA_A$Rs in nRt and VB cells are associated with heterogeneity in subunit expression

The reduction of single $GABA_A$ channel activity in VB neurons by 100 μM Zn^{2+} was significantly larger than that produced in nRt neurons (Fig. 4). This is consistent with recent results obtained using whole cell recordings of acutely isolated thalamic neurons (Gibbs et al. 2000). Our RT-PCR data indicate the presence or absence of subunits but do not describe the stoichiometry of the receptor. This limitation must be kept in mind in interpreting these results. We observed differential expression of α and β subunits in nRt and VB cells. In heterologous systems, three subunits have been shown to have significant roles in Zn^{2+} sensitivity: γ subunits are associated with zinc insensitivity; δ subunits are associated with Zn^{2+} sensitivity, even in the presence of γ subunits (Saxena and MacDonald 1994); and the second transmembrane domain of β subunits has been identified as a Zn^{2+} binding site on the murine $GABA_A$ receptor complex (Wooltorton et al. 1997). VB cells were Zn^{2+} sensitive and yet expressed γ subunits, a finding also reported in a single-cell RT-PCR study of dentate gyrus granule cells (Berger et al. 1998). In fact, our RT-PCR data from native cells showed γ and δ subunits in both nRt and VB neurons. If the Zn^{2+} binding site is on the rat β subunits, as in the mouse, our data would suggest that nRt cells failed to respond to Zn^{2+} due to the low expression of β subunits.

We showed that clonazepam at nanomolar concentrations specifically increases IPSC τ_d in nRt and not VB, while the sIPSC frequency was not affected. Clonazepam enhances recurrent inhibitory strength within the reticular nucleus (Huguenard and Prince 1994b). This results in a decreased ability of neighboring inhibitory neurons to fire synchronously and produce the powerful inhibitory responses required for network synchronization (Huguenard 1999). Our results suggest that enhanced recurrent intra-nRt inhibition produced by clonazepam is due to the slowing of τ_d of IPSCs in individual nRt neurons.

Prior studies examined the effect of a broader range of clonazepam concentrations on GABA responses in acutely isolated neurons. While clonazepam affects the $GABA_A$ currents in both nRt and VB cells, it consistently has a higher potency in nRt cells (Gibbs et al. 1996; Oh et al. 1995). Work from recombinant systems has shown that clonazepam has greater efficacy as a positive modulator of GABA-elicited currents in receptors containing the α3 as opposed to the α1 subunit (Puia et al. 1991; Verdoorn 1994). The pattern of subunit expression we observed in nRt and VB cells did show differences in α1 subunit expression (Tables 2 and 3), suggesting this difference may be relevant to diazepam/clonazepam sensitivity in native systems.

We found evidence of more subunits expressed in the cytosol than are necessary for the formation of a single receptor type, suggesting each cell may have more than one type of $GABA_A$ receptor. Other single-cell RT-PCR studies on $GABA_A$ subunits in native cells have also found supernumerary subunits (e.g., dentate gyrus) (Berger et al. 1998) and evidence for heterogeneity of $GABA_A$ receptors in different portions of individual neurons has been reported in the cerebellum (Brickley et al. 1999; Nusser et al. 1996a). Immunogold localization analysis (Nusser et al. 1996a, 1998) could provide useful data on possible $GABA_A$ receptor heterogeneity within individual VB and nRt cells.

This study provides evidence via RT-PCR for molecular heterogeneity of $GABA_A$ receptors within the thalamus. Molecular heterogeneity has long been suspected as having important consequences for generation and control of thalamic oscillation and processing of sensory information. This has been difficult to directly demonstrate. However, when we combine our kinetic, pharmacological, and RT-PCR analyses in VB and nRt cells with observations from heterologous systems, interesting insights emerge.

Here we provide evidence that α subunit heterogeneity contributes to different IPSC durations in VB and nRt cells. Further, differential expression of α1 versus α3 likely results in differential pharmacology such that inhibitory connections between nRt cells are specifically enhanced by low concentrations of clonazepam. The net effect is an enhanced intra-nRt recurrent inhibition that decreases inhibitory output to VB, an action that can explain the therapeutic effect of clonazepam in absence epilepsy (Huguenard and Prince 1994b). Combined molecular and electrophysiological approaches promise to provide valuable information about the operation of the thalamic networks and selective modulation of circuit activities by existing and new therapeutic agents.

We thank N. Sotelo-Kury for sequencing PCR products and excellent technical assistance and C. L. Cox and D. Ulrich for participating in preliminary experiments critical to this project.

This work was supported by National Institutes of Health Grants NS-06477, NS-34774, NS-07280, and GM-40600 and by the Pimley research and training funds.

REFERENCES

ANGELOTTI TP AND MACDONALD RL. Assembly of $GABA_A$: α1, β2 and $\alpha1\beta1\gamma2$s subunits produce unique ion channel properties with dissimilar single-channel properties. *J Neurosci* 13: 1429–1440, 1993.

ANGELOTTI TP, UHLER MD, AND MACDONALD RL. Assembly of $GABA_A$ receptor subunits: analysis of transient single cell expression utilizing a fluorescent substrate/marker gene combination. *J Neurosci* 13: 1418–1428, 1993.

BENTIVOGLIO M, SPREAFICO R, ALVAREZ-BOLADO G, SANCHEZ MP, AND FAIREN A. Differential expression of the $GABA_A$ receptor complex in the dorsal thalamus and reticular nucleus: an immunohistochemical study in the adult and developing rat. *Eur J Neurosci* 3: 118–125, 1990.

BERGER T, SCHWARTZ C, KRAUSHAAR U, AND MONYER H. Dentate gyrus basket cell $GABA_A$ receptors are blocked by Zn^{2+} via changes of their desensitization kinetics: an *in situ* patch-clamp and single cell PCR study. *J Neurosci* 18: 2437–2448, 1998.

BRICKLEY SG, CULL-CANDY SG, AND FARRANT M. Single-channel properties of synaptic and extrasynaptic $GABA_A$ receptors suggest differential targeting of receptor subtypes. *J Neurosci* 19: 2960–2973, 1999.

CHIANG LW. Detection of gene expression in single neurons by patch-clamp and single-cell reverse transcriptase polymerase chain reaction. *J Chromatogr* 806: 209–218, 1998.

CHIANG LW, SCHWEIZER FE, TSIEN RW, AND SCHULMAN H. Nitric oxide synthase expression in single hippocampal neurons. *Mol Brain Res* 27: 183–188, 1994.

COX CL, HUGUENARD JR, AND PRINCE DA. Cholecystokinin depolarizes rat thalamic reticular neurons by suppressing a K^+ conductance. *J Neurophysiol* 74: 990–1000, 1995.

FRITSCHY JM, BENKE D, MERTENS S, OERTEL WH, BACHI T, AND MOHLER H. Five subtypes of type A gamma-aminobutryic acid receptors identified in neurons by double and triple immunofluorescence staining with subunit-specific antibodies. *Proc Natl Acad Sci USA* 89: 6726–6730, 1992.

FRITSCHY JM AND MOHLER H. $GABA_A$-receptor heterogeneity in the adult rat brain: differential regional and cellular distribution of seven major subunits. *J Comp Neurol* 359: 154–194, 1995.

FRITSCHY JM, PAYSAN J, ENNA A, AND MOHLER H. Switch in the expression of rat $GABA_A$-receptor subtypes during postnatal development: an immunohistochemical study. *J Neurosci* 14: 5302–5324, 1994.

GIBBS JW III, SCHRODER GB, AND COULTER DA. $GABA_A$ receptor function in developing rat thalamic reticular neurons: whole cell recordings of GABA-mediated currents and modulation by clonazepam. *J Neurophysiol* 76: 2568–2579, 1996.

GIBBS JW III, ZHANG YF, SHUMATE MD, AND COULTER DA. Regionally selective blockade of GABAergic inhibition by zinc in the thalamocortical system: functional significance. *J Neurophysiol* 83: 1510–1521, 2000.

GINGRICH KJ, ROBERTS WA, AND KASS RS. Dependence of the $GABA_A$ receptor gating kinetics on the alpha-subunit isoform: implications for structure-function relations and synaptic transmission. *J Physiol (Lond)* 489: 529–543, 1995.

GRANJA R, GUNNERSEN D, WONG G, VALEYEV A, AND SKOLNICK P. Diazepam enhancement of GABA-gated currents in binary and ternary $GABA_A$ receptors: relationship to benzodiazepine binding site density. *J Mol Neurosci* 9: 187–195, 1997.

HAMILL OP, MARTY A, NEHER E, SACKMANN B, AND SIGWORTH BJ. Improved patch-clamp techniques for high-resolution current recording from cells and cell-free membrane patches. *Pflügers Arch* 391: 85–100, 1981.

HOSFORD DA, WANG Y, AND CAO Z. Differential effects mediated by $GABA_A$ receptors in thalamic nuclei in lh/lh model of absence seizures. *Epilepsy Res* 27: 55–65, 1997.

HUGUENARD JR. Neuronal circuitry of thalamocortical epilepsy and mechanisms of antiabsence drug action. *Adv Neurol* 79: 991–999, 1999.

HUGUENARD JR AND PRINCE DA. Intrathalamic rhythmicity studied in vitro: nominal T-current modulation causes robust antioscillatory effects. *J Neurosci* 14: 5485–5502, 1994a.

HUGUENARD JR AND PRINCE DA. Clonazepam suppresses $GABA_B$-mediated inhibition in thalamic relay neurons through effects in nucleus reticularis. *J Neurophysiol* 71: 2576–2581, 1994b.

HUNTSMAN MM AND HUGUENARD JR. Nucleus-specific differences in $GABA_A$-receptor-mediated inhibition are enhanced during thalamic development. *J Neurophysiol* 83: 350–358, 2000.

HUNTSMAN MM, LEGGIO MG, AND JONES EG. Nucleus-specific expression of $GABA_A$ receptor subunit mRNAs in monkey thalamus. *J Neurosci* 16: 3571–3589, 1996.

HUNTSMAN MM, PORCELLO DM, HOMANICS GE, DELOREY TM, AND HUGUENARD JR. Reciprocal inhibitory connections and network synchrony in the mammalian thalamus. *Science* 283: 541–543, 1999.

IM H, IM WB, HAMILTON BJ, CARTER DB, AND VONVOIGLANDER PF. Potentiation of γ-aminobutryic acid-induced chloride currents by various benzodiazepine site agonists with the $\alpha1\gamma2$, $\beta2\gamma$ and $\alpha1\beta2\gamma2$ subtypes of cloned γ-aminobutryic acid type A receptors. *Mol Pharmacol* 44: 886–870, 1993.

JONES EG. *The Thalamus*. New York: Plenum, 1985.

KNOFLACH F, BENKE D, WANG Y, SCHEURER L, LUDDENS H, HAMILTON BJ, CARTER DB, MOHLER H, AND BENSON JA. Pharmacological modulation of the diazepam insensitive recombinant γ-aminobutryic acid receptors $\alpha4\beta2\gamma2$ and $\alpha6\beta2\gamma2$. *Mol Pharmacol* 50: 1253–1261, 1996.

LAURIE DJ, WISDEN W, AND SEEBURG PH. The distribution of thirteen $GABA_A$ receptor subunit mRNAs in the rat brain. III. Embryonic and postnatal development. *J Neurosci* 12: 4151–4172, 1992.

LAVOIE AM, TINGLEY JJ, HARRISON NL, PRITCHETT DB, AND TWYMAN RE. Activation and deactivation rates of recombinant $GABA_A$ receptor channels are dependent on alpha subunit isoform. *Biophys J* 73: 2518–2526, 1997.

MACDONALD RL AND OLSEN RW. $GABA_A$ receptor channels. *Annu Rev Neurosci* 17: 569–602, 1994.

MCKERNAN RM AND WHITING PJ. Which $GABA_A$ receptor subtypes really occur in the brain? *Trends Neurosci* 19: 139–143, 1996.

NUSSER Z, SIEGHART W, BENKE D, FRITSCHY JM, AND SOMOGYI P. Differential synaptic localization of two major gamma-aminobutyric acid type A receptor alpha subunits on hippocampal pyramidal cells. *Proc Natl Acad Sci USA* 93: 11939–11944, 1996a.

NUSSER Z, SIEGHART W, AND SOMOGYI P. Segregation of different $GABA_A$ receptors to synaptic and extrasynaptic membranes of cerebellar granule cells. *J Neurosci* 18: 1693–1703, 1998.

NUSSER Z, SIEGHART W, STEPHENSON FA, AND SOMOGYI P. The alpha 6 subunit of the $GABA_A$ receptor is concentrated in both inhibitory and excitatory synapses on cerebellar granule cells. *J Neurosci* 16: 103–114, 1996b.

OH KS, LEE CJ, GIBBS JW, AND COULTER DA. Postnatal development of $GABA_A$ receptor function in somatosensory thalamus and cortex: whole-cell voltage-clamp recordings in acutely isolated rat neurons. *J Neurosci* 15: 1341–1351, 1995.

PIRKER S, SCHWARZER C, WIESELTHALER A, SIEGHART W, AND SPERK G. $GABA_A$ receptors: immunocytochemical distribution of 13 subunits in the adult rat brain. *Neuroscience* 101: 815–850, 2000.

POULTER MO, BARKER JL, O'CARROLL AM, LOLAIT SJ, AND MAHAN LC. Co-existent expression of $GABA_A$ receptor beta 2, beta 3 and gamma 2 subunit messenger RNAs during embryogenesis and early postnatal development of the rat central nervous system. *Neuroscience* 53: 1019–1033, 1993.

PRITCHETT DB, LUDDENS H, AND SEEBURG PH. Type I and type II GABA-A benzodiazepine receptors produced in transfected cells. *Science* 245: 1389–1392, 1989.

PUIA G, VICINI S, SEEBURG PH, AND COSTA E. Influence of recombinant gamma-aminobutyric acid-A receptor subunit composition on the action of allosteric modulators of gamma- aminobutyric acid-gated Cl^- currents. *Mol Pharmacol* 39: 691–696, 1991.

SAXENA NC AND MACDONALD RL. Assembly of $GABA_A$ receptor subunits: role of the δ subunit. *J Neurosci* 14: 7077–7086, 1994.

SPREAFICO R, DE BIASI S, AMADEO A, AND DE BLAS AL. $GABA_A$-receptor immunoreactivity in the rat dorsal thalamus: an ultrastructural investigation. *Neurosci Lett* 158: 232–236, 1993.

STERIADE M, MCCORMICK DA, AND SEJNOWSKI TJ. Thalamocortical oscillations in the sleeping and aroused brain. *Science* 262: 679–685, 1993.

SUCHER NJ AND DEITCHER DL. PCR and patch-clamp analysis of single neurons. *Neuron* 14: 1095–1100, 1995.

TIA S, WANG JF, KOTCHABHAKDI N, AND VICINI S. Distinct deactivation and desensitization kinetics of recombinant $GABA_A$ receptors. *Neuropharmacology* 35: 1375–1382, 1996.

ULRICH D AND HUGUENARD JR. Purinergic inhibition of GABA and glutamate release in the thalamus: implications for thalamic network activity. *Neuron* 15: 909–918, 1995.

ULRICH D AND HUGUENARD JR. GABA-receptor-mediated rebound burst firing and burst shunting in thalamus. *J Neurophysiol* 78: 1748–1751, 1997.

VERDOORN TA. Formation of heteromeric gamma-aminobutryic acid type A receptors containing two different alpha subunits. *Mol Pharmacol* 45: 475–480, 1994.

VERDOORN TA, DRAGUHN A, YMER S, SEEBURG PH, AND SAKMANN B. Functional properties of recombinant rat $GABA_A$ receptors depend upon subunit composition. *Neuron* 4: 919–928, 1990.

VON KROSIGK M, BAL T, AND MCCORMICK DA. Cellular mechanisms of a synchronized oscillation in the thalamus. *Science* 261: 361–364, 1993.

WISDEN W, LAURIE DJ, MONYER H, AND SEEBURG PH. The distribution of 13 $GABA_A$ receptor subunit mRNAs in the rat brain. I. Telencephalon, diencephalon, mesencephalon. *J Neurosci* 12: 1040–1062, 1992.

WONG G, SEI Y, AND SKOLNICK P. Stable expression of type I γ-aminobutyric acid A/benzodiazepine receptors in a transfected cell line. *Mol Pharmacol* 42: 996–1003, 1992.

WOOLTORTON JR, MCDONALD BJ, MOSS SJ, AND SMART TG. Identification of a Zn^{2+} binding site on the murine $GABA_A$ receptor complex: dependence on the second transmembrane domain of beta subunits. *J Physiol (Lond)* 505: 633–640, 1997.

ZHANG SJ, HUGUENARD JR, AND PRINCE DA. $GABA_A$ receptor-mediated Cl^- currents in rat thalamic reticular and relay neurons. *J Neurophysiol* 78: 2280–2286, 1997.